Mechanism of 4-Chlorobenzoate:Coenzyme A Ligase Catalysis[†]

Rui Wu,[‡] Jian Cao,[‡] Xuefeng Lu,[‡] Albert S. Reger,[⊥] Andrew M. Gulick,[⊥] and Debra Dunaway-Mariano*[,‡]

Department of Chemistry and Chemical Biology, University of New Mexico, Albuquerque, New Mexico 87131, and Hauptman-Woodward Medical Research Institute, Buffalo, New York 14203 and Department of Structural Biology, State University of New York at Buffalo, Buffalo, New York 14203

Received April 21, 2008; Revised Manuscript Received June 4, 2008

ABSTRACT: Within the accompanying paper in this issue (Reger et al. (2008) *Biochemistry*, *47*, 8016−8025) we reported the X-ray structure of 4-chlorobenzoate:CoA ligase (CBL) bound with 4-chlorobenzoyl-adenylate (4-CB-AMP) and the X-ray structure of CBL bound with 4-chlorophenacyl-CoA (4-CP-CoA) (an inert analogue of the product 4-chlorobenzoyl-coenzyme A (4-CB-CoA)) and AMP. These structures defined two CBL conformational states. In conformation 1, CBL is poised to catalyze the adenylation of 4-chlorobenzoate (4-CB) with ATP (partial reaction 1), and in conformation 2, CBL is poised to catalyze the formation of 4-CB-CoA from 4-CB-AMP and CoA (partial reaction 2). These two structures showed that, by switching from conformation 1 to conformation 2, the cap domain rotates about the domain linker and thereby changes its interface with the N-terminal domain. The present work was carried out to determine the contributions made by each of the active site residues in substrate/cofactor binding and catalysis, and also to test the role of domain alternation in catalysis. In this paper, we report the results of steady-state kinetic and transient state kinetic analysis of wild-type CBL and of a series of site-directed CBL active site mutants. The major findings are as follows. First, wild-type CBL is activated by Mg^{2+} (a 12−75-fold increase in activity is observed depending on assay conditions) and its kinetic mechanism (ping-pong) supports the structure-derived prediction that PP_i dissociation must precede the switch from conformation 1 to conformation 2 and therefore CoA binding. Also, transient kinetic analysis of wild-type CBL identified the rate-limiting step of the catalyzed reaction as one that follows the formation of 4-CB-CoA (viz. CBL conformational change and/or product dissociation). The single turnover rate of 4-CB and ATP to form 4-CB-AMP and PP_i ($k = 300\ s^{-1}$) is not affected by the presence of CoA, and it is ∼3-fold faster than the turnover rate of 4-CB-AMP and CoA to form 4-CB-CoA and AMP ($k = 120\ s^{-1}$). Second, the active site mutants screened via steady-state kinetic analysis were ranked based on the degree of reduction observed in any one of the substrate k_{cat}/K_m values, and those scoring higher than a 50-fold reduction in k_{cat}/K_m value were selected for further evaluation via transient state kinetic analysis. The single-turnover time courses, measured for the first partial reaction, and then for the full reaction, were analyzed to define the microscopic rate constants for the adenylation reaction and the thioesterification reaction. On the basis of our findings we propose a catalytic mechanism that centers on a small group of key residues (some of which serve in more than one role) and that includes several residues that function in domain alternation.

In biological systems, carboxylic acids are converted to thioesters, oxygen esters, and amides though a chemical pathway that involves adenylation or phosphorylation of the carboxylic acid reactant by ATP, followed by displacement of the adenylate or phosphate leaving group by the thiol, alcohol or amine coreactant. The enzymes that catalyze such reactions are known as ligases or synthetases. One very large ligase enzyme superfamily (6721 sequence members) is the adenylate-forming family: PFAM00501. Members of this family include firefly luciferase, numerous acyl-CoA synthetases, and the adenylation domains of nonribosomal peptide synthetases (NRPS) (*1*–*3*). The catalytic function common to all members of this enzyme family is the conversion of the substrate carboxylate group to a mixed anhydride via a reaction in which ATP serves as the donor of the adenyl group. The acyl-adenylate formed by luciferase undergoes reaction with molecular oxygen, whereas the acyl-CoA synthetases (also known as acid:CoA ligases) catalyze

[†] This work was supported by NIH Grant NIH GM-36260 to D.D.-M. and by NIH Grant GM-068440 to A.M.G.

* To whom correspondence should be addressed. Tel.: (505) 277-3383. Fax: (505) 277-6202. E-mail: dd39@unm.edu.

[‡] University of New Mexico.

[⊥] Hauptman-Woodward Medical Research Institute and State University of New York at Buffalo.

[1] Abbreviations used are 4-CB, 4-chlorobenzoate; CoA, coenzyme A; CBL, 4-chlorobenzoate: CoA ligase; 4-CB-AMP, 4-chlorobenzoyl-adenosine-5′-monophosphate; 4-CB-CoA, 4-chlorobenzoyl-coenzyme A; PP_i, inorganic pyrophosphate; ATP, adenosine-5′-triphosphate; AMP, adenosine-5′-monophosphate; AMPPNP, adenosine-5′-(β,γ-imido)triphosphate; NADH, β-nicotinamide adenine dinucleotide; PEP, phosphoenol pyruvate; DTT, dithiothreitol; K^+HEPES, potassium salt of *N*-(2-hydroxyethyl)piperzine-*N*′-2-ethanesulfonate; SDS−PAGE, sodium dodecylsulfate−polyacrylamide gel electrophoresis; PheA, the phenylalanine-activating domain of GrsA; NRPS, nonribosomal peptide synthetase (NRPS); 4-MB-AMP, 4-methybenzoyl-adenosine-5′-monophosphate; 4-MB-CoA, 4-methybenzoyl-coenzyme A; 4-CP-CoA, 4-chlorophenacyl-coenzyme A.

10.1021/bi800698m CCC: $40.75
Published on Web 07/12/2008

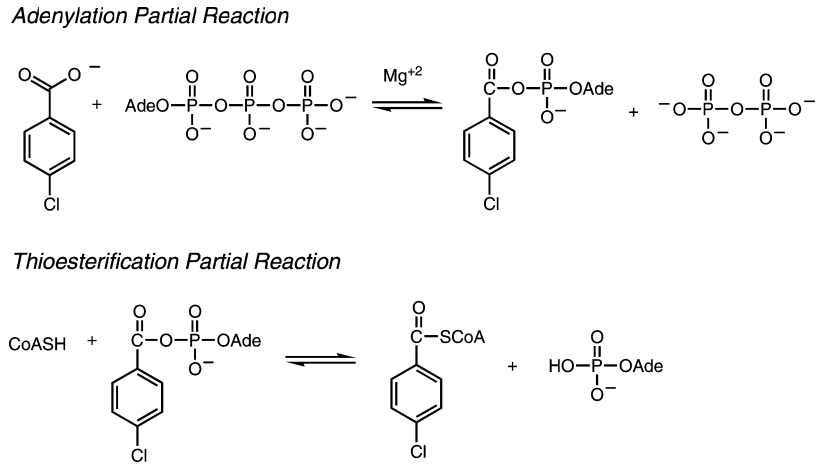

FIGURE 1: The two partial reactions catalyzed by 4-chlorobenzoate:CoA ligase (CBL).

acyl transfer from the acyl-adenylate to the thiol of CoA. The NRPS domains catalyze acyl transfer to the thiol of the pantethiene cofactor that is attached to a peptidyl carrier domain.[1]

Despite the differences in the second partial reactions catalyzed by the enzymes of these three functional subclasses, a two-domain architecture is conserved wherein a large N-terminal core domain is connected to a small C-terminal cap domain by a solvated peptide linker. The active site is formed at the domain-domain interface. X-ray structures of adenylate-forming family members reported to date (*4–14*) evidence the movement of the C-terminal domain through rotation about a hinge region of the solvated linker. This conformational change, termed "domain alternation" (first used to describe the domain motion in the B12-dependent methionine synthase (*15*)), is thought to play an essential role in the catalysis by acetyl-CoA synthetase (*4, 5*) and by 4-chlorobenzoate:CoA ligase (CBL) (*9*), the topic of this paper.

CBL catalysis proceeds via the two partial reactions shown in Figure 1 (*16*). In the accompanying paper in this issue (*17*) we report the X-ray structure of CBL bound with 4-chlorobenzoyl-adenylate (4-CB-AMP) and the X-ray structure of CBL bound with 4-chlorophenacyl-CoA (4-CP-CoA) (an inert analog of the product 4-chlorobenzoyl-coenzyme A (4-CB-CoA)) and AMP. These structures define two CBL conformational states. In conformation 1, CBL is poised to catalyze the adenylation of 4-chlorobenzoate (4-CB) with ATP (partial reaction 1) and in conformation 2 CBL is poised to catalyze the formation of 4-CB-CoA from 4-CB-AMP and CoA (partial reaction 2). The structures show that in switching from conformation 1 to conformation 2, the cap domain rotates about the domain linker and in doing so it changes its interface with the N-terminal domain. In Figure 2 we show the orientation of the C-terminal domain as it is observed in the structure of the CBL(4-CB-AMP) complex (conformer 1) (Figure 2A,B) and the orientation of the C-terminal domain as it is observed in the structure of the CBL(4-CP-CoA) (AMP) complex (conformer 2) (Figure 2C,D). The region of the C-terminal domain (pink) that interfaces with the N-terminal domain (pastel green) in conformer 1 is colored red, and that which interacts with the N-terminal domain in conformer 2 is colored dark green, in order to illustrate the change in the configuration of the active site that occurs when CBL changes from one conformation to the other.

The present work was carried out to determine the contributions made by each of the active site residues (identified through the CBL structure determinations) in the catalysis of the individual partial reactions. The objective was 2-fold: to define the CBL catalytic mechanism and to determine the role of domain alternation in catalysis. In the text below, we report the results from steady-state and transient state kinetic studies of wild-type CBL and of a series of CBL active site site-directed mutants.

MATERIALS AND METHODS

General. All chemicals were purchased from Sigma-Aldrich (St. Louis, MO) except where mentioned. ^{14}C-Labeled 4-chlorobenzoate (specific activity 50−60 mCi/mmol) was obtained from American Radiolabeled Chemicals, Inc. (St. Lous, MO). Custom-synthesized PCR primers were purchased from Invitrogen (Carlsbad, CA) as were the restriction enzymes, the *pfu* polymerase, and the T4 DNA ligase. Competent *Escherichia coli* cells (JM109) were obtained from Stratagene (Cedar Creek, TX) and the pQE-70 vector was purchased from QIAGEN (Valencio, CA). DNA sequence analysis was carried out at the DNA Sequencing Facility of the University of New Mexico. SDS-PAGE analysis was performed with a 12% acrylamide running gel and a 3% stacking gel (37.5:1 acrylamide/biacryamide ratio) (Bio-Rad, Hercules, CA).

Preparation of Wild-Type and Mutant CBL. The His-tagged wild-type CBL was prepared as described in ref *18*. The CBL mutant genes were prepared by PCR by using the *Sph*I-*Bgl*II-pQE-70-CBL clone (*18*) and commercial primers. The purified PCR product was digested with *Sph*I and *Bgl*II (Invitrogen) and ligated to *Sph*I and *Bgl*II digested *Sph*I-*Bgl*II-pQE-70-CBL. The gene sequence was verified by DNA sequencing. A single colony of *E. coli* JM109 cells containing the plasmid *Sph*I-*Bgl*II-pQE-70-CBL was used to inoculate 10 mL of LB medium containing 50 μg/mL ampicillin at 37 °C and 250 RPM. The 10 mL culture was then used to inoculate 10 L of fresh LB medium containing 50 μg/mL ampicillin, and the culture was grown at 20 °C with shaking at 200 RPM. After 26 h (O.D. ~0.7 at 600 nm) IPTG was added to a final concentration of 1 mM. The mixture was incubated at 20 °C and 200 RPM for 10 h, before harvesting

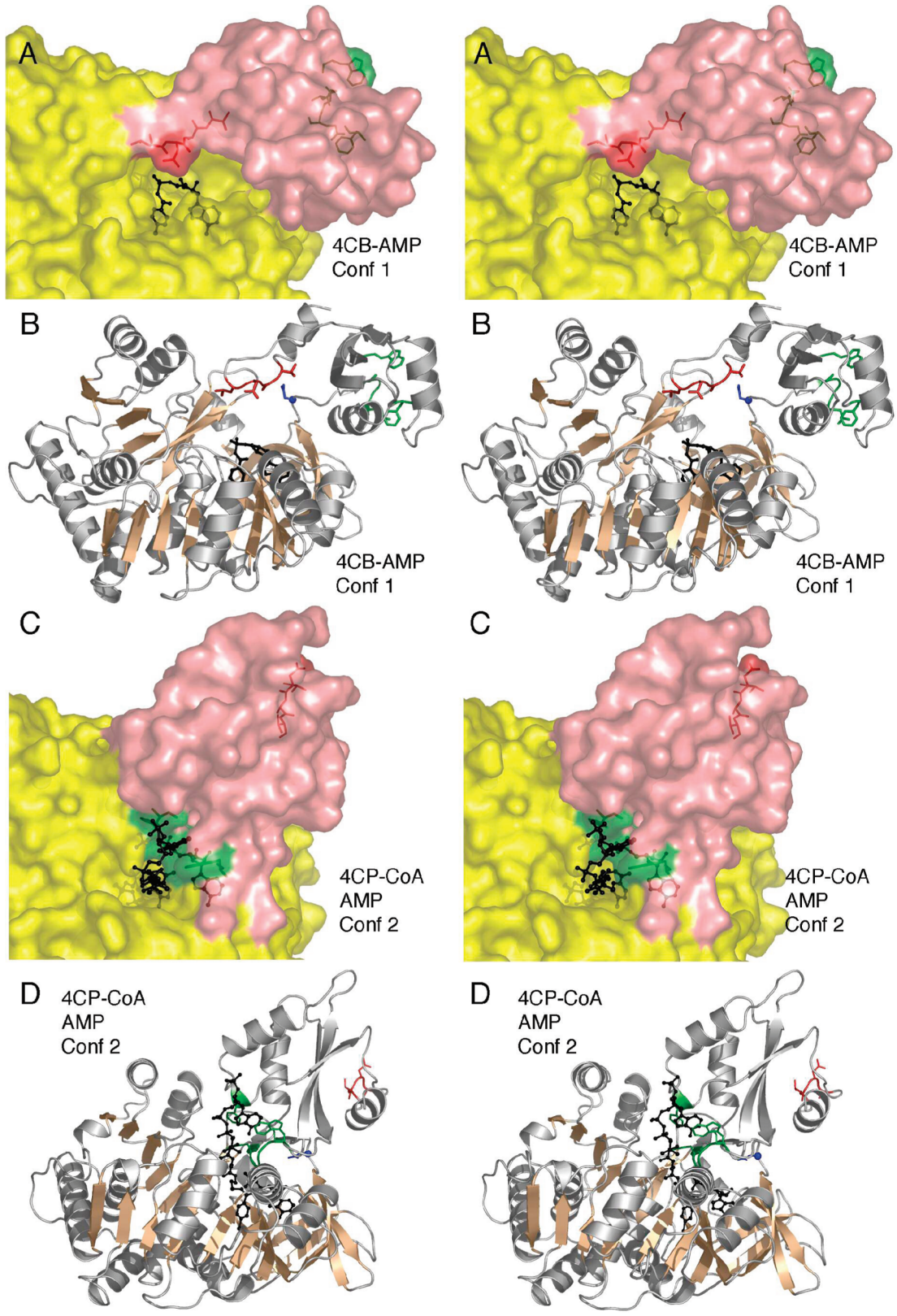

FIGURE 2: The C-terminal domain rotation in CBL based on the crystallographic structures of the CBL conformer 1 bound with 4-CB-AMP (panels A and B) and CBL conformer 2 bound with 4-CP-CoA and AMP (panels C and D) (*17*). In panels A and C, the N-terminal domain is shown in yellow and the C-terminal domain is shown in pink. The surface surrounding residues 490 through 493, which contain the Lys492 residue (disordered beyond Cb) is shown in dark red. These residues are shown in stick formation through the transparent surface. Residues contributing to the active site in conformation 2 are shown in green: Trp440, Phe473, and the A8 loop from Ser407 to Glu410. In panels B and D, the same regions are depicted with stick representation of the side chains. The loops are colored as in A and C, with residues 490−493 shown in red and the Trp440, Phe473, and the A8 loop (Gly399-Gly407) shown in green. Note that in panel C, the A8 loop is not shown in stick format for clarity, however the surface of these residues are colored green. The hinge residue Asp402 is colored blue.

the cells by centrifugation at 5000 × g for 15 min. The 10 g of wet cells were suspended in 100 mL of lysis buffer (50 mM NaH_2PO_4, pH 8.0, 10 mM imidazole, 1 mM DTT) containing 10 μL 0.1 mM protease inhibitor PMSF. The cell suspension was passed through a French press at 1200 PSIG and then centrifuged at 48000 × g and 4 °C for 30 min. The supernatant was loaded onto a Ni-NTA Agarose column (QIAGEN, 25 mL), which had been pre-equilibrated with the lysis buffer. The column was eluted with 500 mL of wash buffer (50 mM NaH_2PO_4, pH 8.0, 50 mM imidazole, 1 mM DTT) and then eluted with 200 mL of elution buffer (50 mM NaH_2PO_4, pH 8.0, 250 mM imidazole, 1 mM DTT). The protein was dialyzed for 3 h against three changes of 1.5 L 50 mM K^+HEPES buffer (pH 7.5) containing 1 mM DTT. The protein purity was verified by SDS-PAGE analysis. The protein concentration was measured by using the Bradford method (*19*) and by measuring the protein solution absorbance at 280 nm ($\varepsilon = 27760\ M^{-1}\ cm^{-1}$). The yields of the CBL mutants ranged from 1 to 7 mg of protein/g of wet cell.

Determination of the Kinetic Mechanism of Wild-Type CBL. The initial velocities were measured for a series of reaction solutions in which the concentration of one substrate (4-methylbenzoate, ATP or CoA) was varied in the presence of different concentrations of a second substrate, while the concentration of the third substrate was held constant at saturating concentration. The reactions were initiated with 0.01 μM wild-type CBL and monitored by using the coupled assay that detects the formation of AMP through the sequential activities of adenylate kinase, pyruvate kinase, and lactate dehydrogenase. The 1 mL solutions initially contained 15 mM $MgCl_2$, 200 μM NADH, 3 mM PEP, 5 mM KCl, 11 U adenylate kinase (EC 2.7.4.3), 9 U pyruvate kinase (EC 2.7.1.40) and 9 U lactate dehydrogenase (EC 1.1.1.27) in 50 mM K^+HEPES (pH 7.5, 25 °C). The decrease in absorbance at 340 nm resulting from the oxidation of two molecules of NADH per molecule of AMP formed was monitored.

The kinetic data were fitted to eqs 1 or 2 using Kaleidagraph,

$$V = V_{max}AB/(K_aB + K_bA + AB) \quad (1)$$

$$V = V_{max}AB/(K_{ia}K_b + K_aB + K_bA + AB) \quad (2)$$

where V is the initial velocity, V_{max} is the maximum velocity, A and B are the concentrations of substrates A and B, K_a and K_b are K_m values for A and B, and K_{ia} is the dissociation constant for EA.

Determination of the Inhibition Constants for CBL Product and Dead-End Inhibitors. 4-Chlorobenzyl-CoA and 4-chlorophenacyl-CoA were prepared as previously described (*17–19*) and tested as inhibitors of CBL catalysis under two sets of conditions: (1) the 4-methylbenzoate concentration was varied at fixed CoA, ATP and $MgCl_2$ concentrations and (2) the CoA concentration was varied at fixed 4-methylbenzoate, ATP and $MgCl_2$ concentrations. AMPPNP, AMPCPP and PP_i were tested as inhibitors of CBL catalysis under the conditions in which the ATP concentration was varied at fixed 4-methylbenzoate, CoA and $MgCl_2$ concentrations. The reactions were initiated with 0.05 μM wild-type CBL and monitored at 25 °C by using the coupled assay that detects the formation of AMP through the sequential activities of adenylate kinase, pyruvate kinase, and lactate dehydrogenase. The 1 mL solutions initially contained 15 mM $MgCl_2$, 200 μM NADH, 3 mM PEP, 5 mM KCl, 11 U adenylate kinase (EC 2.7.4.3), 9 U pyruvate kinase (EC 2.7.1.40) and 9 U lactate dehydrogenase (EC 1.1.1.27) in 50 mM K^+HEPES (pH 7.5, 25 °C). The decrease in absorbance at 340 nm due to the oxidation of two molecules of NADH per molecule of AMP formed was monitored.

AMP was tested as an inhibitor of CBL catalysis under two sets of conditions: (1) the ATP concentration was varied at fixed 4-methylbenzoate, CoA and $MgCl_2$ concentrations and (2) the CoA concentration was varied at fixed 4-methylbenzoate, ATP and $MgCl_2$ concentrations. The reactions were initiated with 0.05 μM wild-type CBL and measured at 25 °C by using a direct continuous spectrophotometric assay wherein the increase in the absorbance of the 1 mL reaction solution resulting from the conversion of 4-methylbenzoate to 4-methylbenzoate-CoA was monitored at 300 nm ($\Delta\varepsilon = 4.1\ mM^{-1}\ cm^{-1}$).

Initial velocity data were analyzed using the program KinetAsyst II (IntelliKinetics, State College, PA) and the equation for competitive inhibition (eq 3), noncompetitive inhibition (eq 4) or uncompetitive inhibition (eq 5).

$$V = V_mS/K_m(1 + I/K_{is}) \quad (3)$$

$$V = V_mS/[K_m(1 + I/K_{is}) + S(1 + I/K_{ii})] \quad (4)$$

$$V = V_mS/[K_m + S(1 + K_{ii})] \quad (5)$$

In these equations, V is the initial velocity, K_m is Michaelis constant of the substrate, K_{ii} is the intercept inhibition constant, K_{is} is the slope inhibition constant, V_m is maximal velocity, and I and S represent the inhibitor and substrate concentrations in the reaction mixture, respectively.

Steady-State Kinetic Constant Determination for CBL Mutants. The CBL activity was measured at 25 °C by using a direct continuous spectrophotometric assay (*9*) wherein the increase in the absorbance of the 1 mL reaction solution resulting from the conversion of 4-chlorobenzoate to 4-chlorobenzoyl-CoA was monitored at 300 nm ($\Delta\varepsilon = 2.5\ mM^{-1}\ cm^{-1}$). The 1 mL assay solutions initially contained ATP, 4-chlorobenzoate, CoA, $MgCl_2$ in 50 mM K^+HEPES (pH 7.5) at 25 °C. For V_{max} and K_m determinations the initial velocity was measured as a function of one substrate concentration (varied from 0.5- to 5-fold K_m) at fixed, saturating concentrations of the cosubstrates. The concentration of "free" Mg^{2+} ([$MgCl_2$] − [ATP]) was constant at 11.5 mM. The initial velocity data were fitted with equation 6 using Kaleidagraph.

$$V = V_m[S]/([S] + K_m) \quad (6)$$

where V is the initial velocity, V_m the maximum velocity, [S] the substrate concentration, K_m the Michaelis constant. The k_{cat} was calculated from the ratio of V_m and enzyme concentration.

Transient-State Kinetics. Single turnover reactions were carried out at 25 °C using a KinTek rapid quench instrument to mix 13 μL of 60 μM wild-type or mutant CBL in 50 mM K^+HEPES (pH 7.5) with 14 μL of 16 μM [^{14}C]4-chlorobenzoate, ATP (7−14 mM as specified), 30 mM $MgCl_2$, and CoA (2−30 mM as specified) in 50 mM K^+HEPES buffer (pH 7.5). Reactions were terminated using 193 μL of 0.1 N HCl as the quench. The reactants and products were separated

by HPLC and quantitated by liquid scintillation counting as described previously (*16, 20*). The rate constants observed for the single-turnover reactions were fitted with the first-order eqs 7 or 8 using Kaleidagraph.

$$[S]_t = [S]_{max} - \left([P]_{max}(1 - e^{-kt})\right) \quad (7)$$

$$[P]_t = [P]_{max}(1 - e^{-kt}) \quad (8)$$

where k is the first-order rate constant; $[S]_t$ and $[P]_t$ are the substrate and product concentrations at time "t", respectively. The rate data collected from the single-turnover reaction with CoA were fitted to a specific kinetic model by using the KINSIM (*21*).

The time course for the multiple turnover reaction catalyzed by wild-type CBL was measured for a reaction solution initially containing 10 μM CBL, 40 μM [^{14}C]4-chlorobenzoate, 500 μM ATP, 500 μM CoA and 12 mM $MgCl_2$ in 50 mM K^+HEPES (pH 7.5). The data were fitted to eq 9 using the program Kaleidagraph.

$$P_t = P_0 - E[A_0(1 - \exp(-(k_1 + k_2)t) + (k_1k_2/(k_1 + k_2))t] \quad (9)$$

where P_t and P_0 are the concentration of the product at time t and zero, E is the final concentration of enzyme active sites, k_1 and k_2 are rate constants of the fast and slow reaction steps in the reaction pathway; k is the first-order rate constant, $[S]_t$ is the substrate concentration at time "t".

RESULTS AND DISCUSSION

Mg^{2+} Dependence of CBL Catalysis. The structure of CBL crystallized in the presence of ATP and 4-chlorobenzoate (4-CB) revealed a 4-CB-AMP ligand bound at the active site of conformer 1 (*17*). This suggested that in the absence of added Mg^{2+} catalytic turnover occurs. The rate of the CBL (11 nM) catalyzed reaction between ATP (3.5 mM), 4-CB (1 mM) and CoA (1 mM) in 50 mM K^+HEPES (pH 7.5, 25 °C) measured in the presence of 15 mM $MgCl_2$ is 0.11 μM s^{-1} and that measured in the absence of added $MgCl_2$ is 0.009 μM s^{-1}. Thus, the Mg^{2+} increases the steady-state rate by a factor of 12. This increase in the turnover rate is comparable to the 15-fold increase in specific activity observed for the propionyl-CoA synthetase from *Salmonella typhimurium* (*22*). A more limited effect has been observed in two additional family enzymes: Mg^{2+} addition resulted in a 2-fold increase in specific activity of the phenylacetate: CoA ligase from *Pseudomonas putida* (*23*) and a 6-fold increase in activity in the *O*-succinylbenzoyl-CoA synthetase of *E. coli* (*24*).

The time course for the single turnover reaction of 30 μM CBL, 15 μM [^{14}C]4-CB and 1 mM ATP in 50 mM K^+HEPES (pH 7.5, 25 °C) was measured (see Materials and Methods for details) in the presence and absence of 15 mM $MgCl_2$ to define the apparent first order rate constants equal to 300 and 4 s^{-1}, respectively. Thus, the added Mg^{2+} increased the rate of 4-CB-AMP formation 75-fold. We conclude that Mg^{2+} is a required cofactor for CBL catalysis. The low activity observed in the absence of added $MgCl_2$ might be attributed to trace contamination of the reaction solution.

The structure of a medium chain acyl-CoA synthetase bound to MgATP was recently deposited in the PDB by the Toronto Structural Genomics Consortium (E. S. Pilka et al., unpublished, PDB accession number 3C5E) to reveal for the first time the Mg^{2+} coordination geometry in a productive complex. This structure shows that the Mg^{2+} is coordinated to the ATP β- and γ-phosphates, and that the Mg^{2+} binds to the equivalent of CBL residue Glu308 via a water ligand. Glu308 is stringently conserved among CBLs and is required for efficient catalysis as evidenced by the reduction in activity observed for the Gln mutant of CBL from *Pseudomonas* sp. strain CBS3 (*20*). Because the Mg^{2+} coordinates to the ATP and not to the ligase, we presume that it enters the active site coordinated with the ATP and following catalytic turnover departs the active site coordinated with the PP_i.

The CBL Kinetic Mechanism. The CBL catalyzed conversion of 4-CB to 4-CB-CoA requires that the 4-chlorobenzoate displaces PP_i from the α-P of ATP, and that CoA then displaces AMP from the 4-CB-AMP intermediate (Figure 1). There is no indication from the CBL structures reported in the previous paper that the substrate binding sites are overlapping. Thus, a sequential kinetic mechanism in which all three reactants bind to the enzyme prior to product formation may be anticipated. Yet in the previous paper (*17*) we have provided structural evidence that the C-terminal domain, which adopts conformation 1 for the reaction of ATP with 4-chlorobenzoate, must rotate 140° to conformation 2 in order to catalyze the thioesterification reaction (see Figure 2). As will be detailed later in the text, the CoA binding site is obstructed (by His207) in conformation 1 and the switch from conformation 1 to 2 requires the dissociation of PP_i (in order to vacate the site for Asn411). This sequence of events may be best represented by a ping-pong kinetic mechanism. Experimentally, the ping-pong and sequential mechanisms are distinguished by the patterns of the double reciprocal initial velocity plots.

Accordingly, the initial velocity of (Mg^{2+} activated) CBL catalyzed conversion of 4-methylbenzoate[2], ATP, and CoA to PP_i, 4-methylbenzoyl-CoA (4-MB-CoA), and AMP was measured as a function of substrate concentration. The concentrations of two substrates were varied and the concentration of the third substrate was held constant. The double reciprocal plots of the initial velocity data are presented in Figure 3. Two of the plots (Figure 3A,B) define parallel lines whereas the third (Figure 3C) defines intersecting lines. These results show that whereas ATP and 4-chlorobenzoate bind to enzyme forms that are reversibly connected, CoA and ATP or CoA and 4-chlorobenzoate do not. The irreversible step is the result of PP_i dissociation prior to CoA binding. We conclude that CBL catalysis occurs via the Bi Uni Uni Bi ping-pong kinetic mechanism shown in Figure 4. "Ping-pong kinetics" have also been reported for malonyl-CoA synthetase (*25*), acyl-CoA synthetases (*26, 27*), and propionyl-CoA synthetase (*22*).

The Rate-Limiting Step in CBL Catalysis Follows the Formation of 4-CB-CoA. CBL catalysis involves numerous substrate binding and product release steps in addition to the chemical steps associated with CB-AMP formation and transformation to CB-CoA (Figure 4). In order to determine

[2] The 4-methylbenzoate (K_m = 18 μM) was used in place of 4-chlorobenzoate because the K_m for 4-chlorobenzoate is so small (~1 μM) that it is difficult to measure the small amount of product generated from 4-chlorobenzoate at the required concentration range (0.5 to 5K_m).

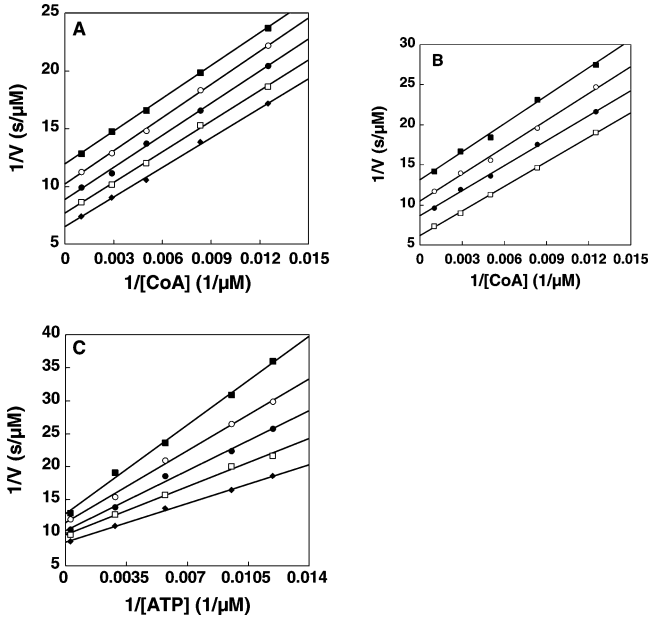

FIGURE 3: Initial velocity patterns for CBL reaction. (A) Plots of $1/V$ versus 1/[CoA] at various concentrations of 4-methylbenzoate and at a constant concentration of ATP (3.5 mM). 4-Methylbenzoate concentrations used are 20 μM (■), 40 μM (○), 60 μM (●), 80 μM (□), and 100 μM (♦). (B) Plots of $1/V$ versus 1/[CoA] at various concentrations of ATP and at a constant concentration of 4-methylbenzoate (200 μM). ATP concentrations used are 105 μM (■), 175 μM (○), 350 μM (●), and 875 μM (□). (C) Plots of $1/V$ versus 1/[ATP] at various concentrations of 4-methylbenzoate and at a constant concentration of CoA (1 mM). 4-Methylbenzoate concentrations used are 20 μM (■), 40 μM (○), 60 μM (●), 80 μM (□) and 100 μM (♦). The data of A and B were fitted to eq 2 and the apparent values for the kinetic constants were obtained as follows: $k_{cat} = 8.0 \pm 0.6$ s^{-1}, K_M (4-methylbenzoate) $= 30 \pm 5$ μM, K_M (CoA) $= 160 \pm 20$ μM at 3.5 mM ATP; $k_{cat} = 8.2 \pm 0.3$ s^{-1}, K_M (CoA) $= 190 \pm 14$ μM, K_M (ATP) $= 180 \pm 15$ μM at 200 μM 4-methylbenzoate. The data of C were fitted eq 1 to define $k_{cat} = 6.3 \pm 0.4$ s^{-1}, K_M (4-methylbenzoate) $= 14 \pm 4$ μM, K_M (ATP) $= 80 \pm 20$ μM at 1 mM CoA.

if a chemical step is rate limiting we measured the time course for the first few turnovers. The initial reaction solution consisted of 10 μM wild-type CBL, 40 μM [^{14}C]4-CBA, 500 μM ATP, 500 μM CoA and 12 mM $MgCl_2$ in 50 mM K$^+$HEPES (pH 7.5). The time course displays an obvious burst of ~10 μM 4-CB-CoA followed by a slower, steady-state rate of 4-CB-CoA formation (Figure 5). This result indicates fast transformation of the enzyme−substrate complex to the enzyme−product complex (k_1) followed by a comparatively slower rate of regeneration of the catalytically active form of the enzyme (k_2). The rate data were fitted to eq 9 to give k_1 for the burst phase as 60 ± 10 s^{-1} and $k_2 = 10.2 \pm 0.7$ s^{-1} for subsequent turnovers. The k_2 is in accordance with the k_{cat} (12 s^{-1}) of the wild-type CBL catalyzed reaction. Slow 4-CB-CoA release and/or the switch from conformation 2 to conformation 1 (Figure 2) might therefore, be the rate-determining step of CBL catalysis.

Inspection of the surfaces of the CBL complex of 4-CB-AMP in conformation 1 and of the 4-chlorophenacyl-CoA (4-CP-CoA) in conformation 2 (Figure 2) suggests that the dissociation of the product ligands AMP and 4-CB-CoA may not occur from conformation 2 because they are buried. In particular, the greater solvent exposure of the AMP in conformation 1 would facilitate its dissociation and thus, a probable scenario is one in which the second chemical step is followed by a conformational change that is required for the dissociation of both products.

Dead-End and Product Inhibition of CBL Catalysis. The ATP analogs AMPPNP and AMPCPP were tested as inhibitors vs ATP (200 μM CoA and 20 μM 4-methylbenzoate) and surprisingly no inhibition was observed at the K_m level of ATP and 5 mM inhibitor (nor are these analogs CBL substrates). AMPPNP and AMPCPP were also tested as inhibitors of the *Salmonella* acetyl-CoA synthetase with the same result. The weak binding may account for why attempts to obtain crystals of these two enzymes with a bound AMPPNP or AMPCPP ligand have failed, yet the reason why these enzymes discriminate against these analogs is unclear. In particular, the structure of the CBL(4-CB-AMP) complex shows multiple binding interactions between the AMP unit and the residues that line its binding pocket (see discussion below). In addition, the structure of the human medium chain acyl-CoA synthetase bound with MgATP (PDB accession code 3C5E) shows that a P-loop (conserved in the family) binds the ATP γ-phosphate and that the Mg^{2+} cofactor binds the ATP β- and γ-phosphates. In the present work we have found that CBL binds both AMP and PP_i with reasonable affinity. Specifically, AMP is a noncompetitive inhibitor vs ATP: $K_{is} = 120 \pm 20$ μM; $K_{ii} = 600 \pm 60$ μM (200 μM CoA and 20 μM 4-methylbenzoate; Supporting Information, Figure SI1A) and an uncompetitive inhibitor vs CoA: $K_{ii} = 250 \pm 10$ μM (200 μM ATP and 20 μM 4-methylbenzoate; Supporting Information, Figure SI1B) and PP_i is a competitive inhibitor vs ATP: $K_{is} = 95 \pm 10$ μM (200 μM CoA and 20 μM 4-methylbenzoate; Supporting Information, Figure SI1C). The only explanation for the weak CBL binding of AMPCPP and AMPPNP that we can offer at this time is that substitution of a bridge oxygen atom with "CH_2" or "NH" alters the conformation of the tripolyphosphate chain to the extent that favorable interactions with the CBL P-loop (residues 161−166) and/or the Mg^{2+} cofactor are precluded.

The product analog 4-chlorophenacyl-CoA (4-CP-CoA), used in the structure determination of CBL in conformation 2 (*17*), was tested as a dead-end inhibitor vs CoA (200 μM ATP, 20 μM 4-methylbenzoate) and vs 4-methylbenzoate (300 μM CoA, 200 μM ATP) in order to assess its binding affinity. In both cases noncompetitive inhibition was observed to define $K_{is} = 21 \pm 8$ μM and $K_{ii} = 25 \pm 3$ μM and $K_{is} = 30 \pm 8$ μM and $K_{ii} = 24 \pm 2$ μM, respectively (Supporting Information, Figures SI1D and SI1E). The closely related analog 4-chlorobenzyl-CoA (wherein the benzoyl C=O is replaced with CH_2) was also found to be a noncompetitive inhibitor vs CoA and vs 4-methylbenzoate (Supporting Information, Figures SI1F and SI1G): $K_{is} = 45 \pm 10$ μM and $K_{ii} = 40 \pm 3$ μM and $K_{is} = 14 \pm 3$ μM and $K_{ii} = 19 \pm 2$ μM, respectively. The tight binding observed for the two product analogs is consistent with the multiple binding interactions between the 4-CP-CoA and the enzyme, as is evidenced by the CBL(4-CP-CoA) structure (see discussion below).

A Profile of Active Site Residues Derived from Steady-state Kinetic Analysis of Site-directed Mutants. The structures of the CBL complex of 4-CB (conformation 1), the CBL complex of 4-CB-AMP (conformation 1), and the CBL complex of 4-CP-CoA (conformation 2) provide snap shots of the interaction of the enzyme with the chemical species

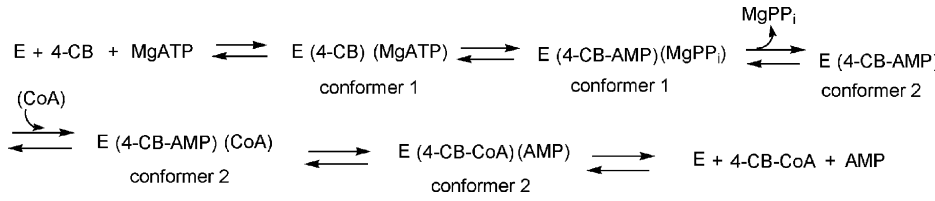

FIGURE 4: The proposed kinetic mechanism of the CBL catalyzed conversion of 4-CB, ATP and CoA to 4-CB-CoA, AMP and PP_i.

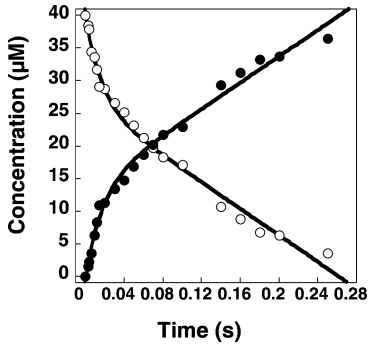

FIGURE 5: The time course for the first few catalytic turnovers of 4-CB, ATP and CoA, as plotted as 4-CB-CoA concentration vs reaction time. The initial reaction solution consisted of 10 μM wild-type CBAL, 40 μM [^{14}C]4-CBA, 500 μM ATP, 500 μM CoA and 12 mM $MgCl_2$ in 50 mM K^+Hepes (pH 7.5). The data were fitted to eq 8 for the multiple turnover reaction using the Kaleidagraph program giving the k_1 for the burst phase 60 $\pm$ 10 s^{-1} and for the following turnovers k_2 = 10.2 $\pm$ 0.7 s^{-1}.

formed along the reaction coordinate. As the reaction progresses from the central reactant CBL(4-CB)(ATP) to the central product complex CBL(4-CB-CoA)(AMP) via the CBL(4-CB-AMP)(PP_i) intermediate, different enzyme residues are recruited to participate. The snap shots of CBL catalysis provided by the crystal structures identify the enzyme residues that are positioned to function in substrate binding and/or catalysis (see Figure 6A−C), yet they do not define the contribution of the suggested interaction to the catalytic efficiency. Here we report the results of the steady-state kinetic analyses of CBL active site mutants. The goal of this kinetic study is to distinguish between residues that are playing spectator roles in catalysis (i.e., are close enough to interact with the reactant but do not significantly reduce the energy barrier) from those whose participation is required.

Table 1 lists the ATP, 4-CB and CoA k_{cat}/K_m values measured for wild-type and mutant CBLs (the k_{cat} and K_m values are reported in Table SI1, Supporting Information). The k_{cat}/K_m values reflect the efficiency of CBL catalysis of the full reaction under conditions where the concentration of the target substrate is not saturating and the concentrations of the two cosubstrates (and the Mg^{2+} activator) are saturating. We considered a difference in the wild-type and mutant CBL k_{cat}/K_m values that exceeds a 50-fold decrease as sufficient to classify the mutated residue as one required for CBL catalysis. Mutants that displayed smaller decreases in k_{cat}/K_m values were not subjected to further investigation.

The residues that surround the 4-CB reactant are shown in Figure 6A. The 4-CB chlorinated ring fits snuggly in a hydrophobic pocket. In previous work we explored the contributions made by the binding pocket residues (*18*). The 4-CB carboxylate group projects outside of the hydrophobic pocket where it is close to, but not within interaction distance of, the side chains of stringently conserved CBL residues Lys492 and His207. Because both of these residues are mobile, the still picture provided by the crystal structure may not show these residues in the exact location that they occupy during catalytic turnover. Specifically, the His207 side chain is seen in a rotomer conformation in CBL conformer 1 (χ_1 = −166°, Figure 6A,B) that is different from the rotomer conformation observed in CBL conformer 2 (χ_1 = −60°, Figure 6C). The His207 imidazole ring N3 atom is located 3.7 Å away from the carboxylate group of 4-CB in the CBL(4-CB) structure yet is observed to form a hydrogen bond with the scissile ester oxygen atom of the 4-CB-AMP ligand in the CBL(4-CB-AMP) structure. This latter structure suggests that His207 interacts with the 4-CB carboxylate group during catalysis of the first partial reaction. The His207 side chain conformation observed in conformer 1 places the His207 ring in the path of the CoA pantetheine arm. Therefore, in order for CoA to bind to CBL, the His207 side chain must move, which it does when CBL conformer 1 switches to conformer 2 (see Figure 6D). The H207A mutant 4-CB k_{cat}/K_m value is reduced 500-fold whereas the ATP and CoA k_{cat}/K_m values are not as greatly reduced.

Lys492 is stringently conserved within the family. Structural data and mutagenesis data reported for several family members evidence a required role for the Lys in binding the substrate carboxylate group (*28*), surfactin synthetase (*29*), propionyl-CoA (*22*), and acetyl-CoA synthetase (*5*). Figure 2 depicts the movement of Lys492 between the active site and the solvent as CBL switches between conformation 1 and conformation 2. In conformation 1 the Lys492 ammonium group is not quite close enough to the 4-CB carboxylate group for ion pair formation (Figure 6A). We have noted (*6*) however, that the CBL structures depict a slightly more "open" domain-domain interface for conformation 1 than has been observed in the structures of other family members. Indeed, only a slight rotation of the CBL C-terminal domain is needed to correctly position the Lys492 for interaction with the 4-CB carboxylate group. From inspection of Table 1, it is evident that the replacement of the Lys492 in CBL with Arg, Leu, or Ala has the greatest impact on the 4-CB k_{cat}/K_m value (300, 2000, and 500-fold reduction, respectively). This is consistent with the interaction of Lys492 with the 4-CB carboxylate group during catalytic turnover. This interaction might also be important for stabilizing the enzyme in conformation 1 long enough for catalysis of the first partial reaction to occur. Once the 4-CB-AMP product is formed (thereby destroying the original ion pair) the C-terminal domain may freely rotate to form conformation 2.

The side chain of Thr307 is seen in the CBL(4-CB-AMP) structure to engage in a hydrogen bond interaction with one of the oxygen atoms of the nucleotide α-phosphate (Figure 6B). The corresponding Thr (T326, T327, T416, and T472, respectively) is observed in crystal structures of PheA, ttLC-FACS and the acetyl CoA synthetases from *Salmonella*

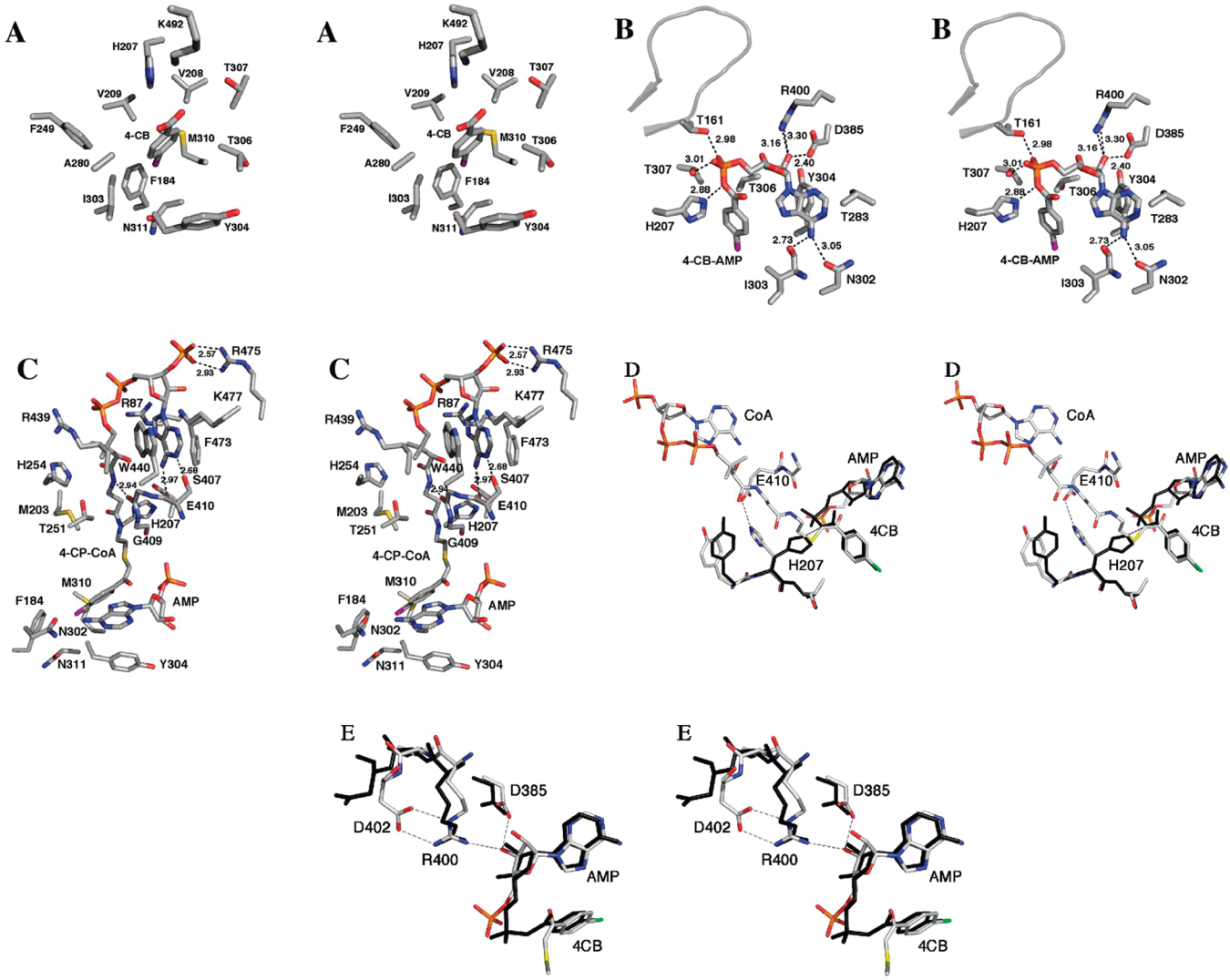

FIGURE 6: Stereodiagrams of the CBL binding site residues surrounding (A) the 4-CB in CBL(4-CB) complex in conformation 1, created using the X-ray crystallographic coordinates deposited as PDB accession IDs 1T5D (CBL bound to 4-CB) and 2qw0 (I303A CBL mutant bound to 3,4-dichlorobenzoate, in which residue K492 side chain is ordered), (B) the nucleotide unit of 4-CB-AMP in the CBL(4-CB-AMP) complex in conformation 1, and (C) the 4-CP-CoA and AMP in the CBL(4-CP-CoA)(AMP) complex in conformation 2. (D) A superposition of the two conformational states of CBL are shown. Atoms from conformation 2 are shown with colored atoms while the atoms from conformation 1 are shown in black. Glu410 is not shown for conformation 1 as it is positioned >20 Å from the active site. The three subpockets of the active site are labeled AMP, 4-CB, and CoA. (E) Superposition of the loop at residues Arg400-Asp402 that interact with AMP in the two conformations. The 4-CP-CoA inhibitor is truncated at the first carbon of the pantetheine group. The figures were created by using PYMOL.

enterica and yeast to engage in hydrogen bond formation with the α-phosphate of AMP. The Thr307 is replaced with Ser in two CBLs, however the hydroxyl group is preserved. The Thr homologue is also observed in other family members with the exception of DhbE, which has an Ala at the corresponding position. The mutation of this Thr (T307) in firefly luciferase (T343) to alanine (*30*) was shown to reduce the turnover rate 120-fold. Replacement of CBL Thr307 with Ala resulted in a significant (100-fold) reduction in the 4-CB k_{cat}/K_m value with a comparably smaller impact on the ATP (20-fold reduction) and CoA (2-fold reduction) k_{cat}/K_m values.

Thr161, which is the first residue of the conserved "P-loop" (see below), is suggested by the CBL(4-CB-AMP) structure to engage in a hydrogen bond interaction with one of the oxygen atoms of the nucleotide α-phosphate (Figure 6B). Furthermore, the structure of the human medium chain acyl-CoA synthetase(MgATP) complex (PDB accession number 3C5E) demonstrates numerous interactions between the P-loop and the ATP γ-phosphate which include the main chain amides of the counter parts to CBL residues Gly163 and Thr165, and the side chain hydroxyls of the counter parts to P-loop residues Thr161 and Thr165. The replacement of CBL Thr161 with Ala resulted in a large decrease in the ATP and 4-CB k_{cat}/K_m values and a comparatively small decrease in the CoA k_{cat}/K_m value (Table 1). In previous work (*20*), kinetic analysis of *Pseudomonas* sp. strain CBS3 CBL P-loop mutants G163I, G166I and P168A evidenced the important role of the P-loop in catalysis of the first partial reaction.

The residues that interact with the adenosine unit of the CBL bound 4-CB-AMP ligand (Figure 6B) include Asn302 (forms a hydrogen bond with the C(6)NH_2) and Tyr304 (stacks against the adenine ring), Arg400 (forms a hydrogen bond with the 2′-hydroxyl group of the ribose ring) and Asp385 (forms a hydrogen bond with the 2′-hydroxyl group of the ribose ring). Asn302 (replaced by Asp in some CBLs),

Table 1: The Steady-State Kinetic Constants Measured for CBL Catalysis in 50 mM K^+ HEPES (pH 7.5, 25 °C)[a]

enzyme	substrate	k_{cat}/K_m (M^{-1} s^{-1})	X-fold decrease	enzyme	substrate	k_{cat}/K_m (M^{-1} s^{-1})	X-fold decrease
W.T.	4-CB	1×10^7		E410A	4-CB	2×10^5	50
	CoA	6×10^4			CoA	4×10^1	1000
	ATP	1×10^5			ATP	2×10^3	50
K492A	4-CB	2×10^4	500	G408A	4-CB	2×10^5	50
	CoA	4×10^4	0		CoA	2×10^3	20
	ATP	2×10^3	50		ATP	4×10^3	20
K492L	4-CB	6×10^3	2000	M203A	4-CB	2×10^5	50
	CoA	2×10^4	3		CoA	5×10^3	10
	ATP	9×10^2	100		ATP	8×10^3	10
K492R	4-CB	3×10^4	300	H254A	4-CB	4×10^5	20
	CoA	3×10^4	2		CoA	2×10^3	30
	ATP	2×10^3	50		ATP	8×10^3	10
H207A	4-CB	2×10^4	500	T251A	4-CB	2×10^6	5
	CoA	6×10^3	10		CoA	7×10^3	10
	ATP	6×10^3	20		ATP	2×10^4	5
H207Q	4-CB	3×10^4	300	R475A	4-CB	3×10^5	30
	CoA	6×10^3	10		CoA	9×10^3	7
	ATP	6×10^2	200		ATP	1×10^4	10
H207F	4-CB	6×10^5	20	K477A	4-CB	5×10^5	20
	CoA	2×10^4	3		CoA	5×10^3	10
	ATP	5×10^4	2		ATP	3×10^4	3
R400A	4-CB	1×10^5	100	R439A	4-CB	6×10^6	2
	CoA	1×10^2	600		CoA	1×10^4	6
	ATP	1×10^3	100		ATP	7×10^4	0
D385A	4-CB	2×10^4	500	R87A	4-CB	2×10^6	5
	CoA	2×10^4	3		CoA	3×10^4	2
	ATP	2×10^2	500		ATP	3×10^3	30
T306A	4-CB	2×10^5	50	F473A	4-CB	1×10^6	10
	CoA	4×10^4	0		CoA	1×10^2	600
	ATP	1×10^4	2		ATP	4×10^4	2
T307A	4-CB	8×10^4	100	N302A	4-CB	1×10^6	10
	CoA	3×10^4	2		CoA	3×10^4	2
	ATP	4×10^3	20		ATP	9×10^3	10
T161A	4-CB	5×10^3	2000	Y304F	4-CB	4×10^6	2
	CoA	1×10^4	6		CoA	8×10^4	0
	ATP	4×10^1	2000		ATP	7×10^4	0
S407A	4-CB	4×10^6	2	W440A	4-CB	4×10^5	20
	CoA	1×10^2	600		CoA	1×10^2	600
	ATP	4×10^4	2		ATP	1×10^4	10

[a] Reaction solutions contained saturating concentrations of Mg^{+2} and the two co-substrates (see Materials and Methods for details). The k_{cat} and K_m values are reported in Supporting Material, Table SI1.

Tyr304 (stringently conserved among CBLs) and Asp385 (replaced by Ala in one CBL) are located on the N-terminal domain whereas Arg400 (stringently conserved among CBLs) immediately precedes the domain-domain linker "hinge region" (defined by the blue colored Asp402 in Figure 2B,D). Replacement of Tyr304 with Phe conserves the potential for ring stacking with the adenine ring in the Y304F mutant, which is notably, fully active (Table 1). In contrast, Y304A CBL failed to fold properly as indicated by its formation of an inclusion body. The N302A mutant is only 10-fold less active than wild-type CBL which indicates that the hydrogen bond with the C(6)NH_2 does not contribute significantly to catalysis. The ATP and 4-CB k_{cat}/K_m values are significantly reduced (500-fold) in the D385A mutant whereas the CoA k_{cat}/K_m value is not. The k_{cat}/K_m values for 4-CB, ATP and CoA are significantly reduced in the R400A mutant.

The residues that surround the CoA ligand (Figure 6C) include Met203, Thr251, His254, Gly408, Gly409, Ser407, Phe473, Trp440, Arg475, Lys477, Arg439, and Arg87. Met203, Thr251, His254, Gly408, and Gly409. In the case of Gly408 and Gly409 of the A8 loop (shown as the green "stick" region in Figure 2B) hydrogen bond formation takes place between the main chain carbonyls and the amide NHs of the CoA pantetheine 4-CP-CoA ligand. The two corresponding residues in the *Salmonella* acetyl-CoA synthetase S523 and G524 play similar roles. In the case of acetyl-CoA synthetase, the G524L mutant catalyzes the adenylation reaction but not the thioesterification reaction (*5*). Unfortunately, mutation of the CBL Gly409 to Leu (the create the CBL homologue to the *Salmonella* acetyl-CoA synthetase G524L mutant) resulted in insoluble protein. The G408A CBL mutant was, however successfully prepared and shown to have only modest reductions in the k_{cat}/K_m values (Table 1). However, this is not surprising given that it is the Gly408 backbone C═O that binds the CoA and that the additional steric bulk provided by the methyl side chain of the Ala mutant may be too small perturb this interaction. The side chains of Met203, Thr251 and His254 that line the "pantetheine tunnel" (Figure 2D) do not directly interact with the ligand, nor do they make a significant contribution to the catalytic efficiency (Table 1).

The side chain of Ser407 is within hydrogen bond forming distance of the CoA C(6)NH_2 whereas the Phe473 and Trp440 line the shallow hydrophobic crevice which accommodates the CoA adenine ring. Ser407 is conservatively replaced by Thr in some CBLs whereas Phe473 and Trp440 are stringently conserved. The corresponding Ala mutants display a 600-fold reduction in the CoA k_{cat}/K_m value, and comparatively small reductions in the 4-CB and ATP k_{cat}/K_m values.

The charged groups observed in the crystal structure of the CBL(4-CP-CoA) complex to interact with CoA are the side chains of Arg475 (forms an ion pair with the CoA 3′-phosphate), Lys477 (forms a hydrogen bond with the CoA adenine ring N3), Arg439 (located near the CoA β-phosphate), and Arg87 (forms an ion pair with the CoA α-phosphate) (Figure 6C). It is striking that the substitution of each of the residues with Ala has an insignificant impact on the catalytic efficiency of CBL (Table 1). On the other hand, the interactions are occurring at the protein surface (see Figure 2C,D) and therefore, in a water solvent environment. Weak binding of the nucleotide unit of CoA at the protein−solvent interface has been noted for enzymes that act on acyl-CoA substrates (31−32).

Perhaps the most interesting residue found in the vicinity of the CoA is Glu410. This residue, which is stringently conserved among CBLs, does not interact with the ligand in the CBL(4-CB-AMP) structure nor in the CBL(4-CP-CoA) structure but it does bind the His207 side chain in the CBL(4-CP-CoA) structure (conformation 2) (see Figure 6D). The E410A mutant experiences a 1000-fold reduction in the CoA k_{cat}/K_m value and comparatively small decreases in the 4-CB and ATP k_{cat}/K_m values.

The residues thus identified as making significant contributions to CBL catalytic efficiency were subjected to further investigation for the purpose of defining their participation in one, or both of the two partial reactions. These experiments are described in the following section.

A Dissection of the Contributions of the Active Site Residues to Catalysis of the Individual Partial Reactions. Here we report the results from transient state kinetic analysis of the two CBL partial reactions. First, the rates of the conversion of CBL(4-CB)(ATP) to CBL(4-CB-AMP)(PP_i) catalyzed by wild-type and mutant CBLs were measured. This was accomplished by carrying out single turnover reactions of [^{14}C]4-CB and ATP (in the absence of CoA) and measuring the time courses for [^{14}C]4-CB consumption and [^{14}C]4-CB-AMP formation. The reactions were carried out using CBL (29 μM) in excess to [^{14}C]4-CB (8.3 μM) to ensure that all of the [^{14}C]4-CB was bound to the enzyme. The ATP (3.5−7.0 mM) and Mg^{2+} (16 mM) were present at saturating concentrations. The time course for the single turnover reaction catalyzed by wild-type CBL is shown in Figure 7A. The data were fitted to a single exponential to define an apparent first order rate constant $k_{obs} = 270 \pm 10$ s^{-1}. The process was repeated using double the concentration of CBL (60 μM) to define $k_{obs} = 330 \pm 60$ s^{-1}. The observation that the rate is independent of the CBL concentration indicates that, under the conditions employed to measure the single turnover rates, substrate binding is not rate limiting. Thus, the value of k_{obs} defines the rate at which CBL(4-CB)(ATP) converts to CBL(4-CB-AMP)(PP_i). The ratio of the [^{14}C]4-CB-AMP and [^{14}C]4-CB observed at the completion of the single turnover reaction is an approximation of the internal equilibrium constant $^{int}K_{eq}$ = CBL(4-CB-AMP)(PP_i)/CBL(4-CB)(ATP). The time course measured for wild-type CBL suggests that $^{int}K_{eq}$ is greater than or equal to 10.

Second, the single turnover reactions of [^{14}C]4-CB, ATP and CoA were carried out under the same conditions used for analysis of the first partial reaction, except that CoA was included at a saturating concentration. The time courses for

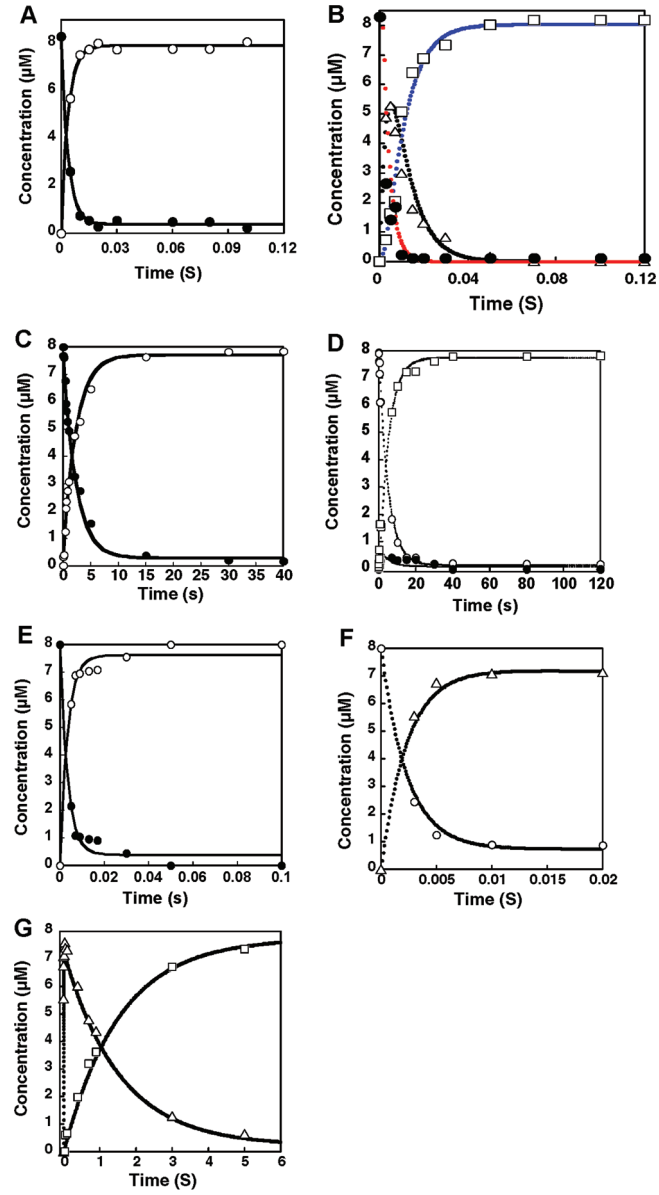

FIGURE 7: Time course for CBL catalyzed single turn over reaction in 50 mM K^+ HEPES (pH 7.5, 25 °C). The final concentration of the reactants in the 27 μL reaction mixture were 8.3 μM 4-CB and 15.6 mM $MgCl_2$ and (A) 29 μM wild type CBL with 3.5 mM ATP; (B) 29 μM wild type CBL with 1 mM CoA, 3.5 mM ATP; (C) 29 μM K492A CBL with 7 mM ATP; (D) 29 μM K492A CBL with 1 mM CoA, 7 mM ATP; (E) 29 μM W440A CBL with 3.5 mM ATP; (F, G) 29 μM W440A CBL with 16 mM CoA, 3.5 mM ATP. The rate data measured for the full reaction were fitted to the kinetic model shown in Scheme 1 using KINSIM (*21*). The microscopic rate constants are reported in Table 2 and 3. The reaction curves are as follows: (A) 4-CB (●), 4-CB-AMP (○); (B) 4-CB (●), 4-CB-AMP (△), 4-CB-CoA (□); (C) 4-CB (●), 4-CB-AMP (○); (D) 4-CB (○), 4-CB-AMP (●), 4-CB-CoA (□); (E) 4-CB (●), 4-CB-AMP (○); (F, G) 4-CB (○), 4-CB-AMP (△), 4-CB-CoA (□).

Scheme 1

[^{14}C]4-CB consumption, [^{14}C]4-CB-AMP formation and consumption, and [^{14}C]4-CB-CoA formation were measured and analyzed using the kinetic model shown in Scheme 1, and the simulation program KINSIM (*21*) (Figure 7B). These microscopic rate constants defined by the time course simulations are reported in Table 3, along with the percent

Table 2: The Observed First-Order Rate Constants (k_{obs}) Derived from Single Turnover Time Course Data (Shown in Figure SI1 of Supporting Information) for the Reaction of 8.3 μM [^{14}C]4-Chlorobenzoate (4-CB) with 29 μM Wild-Type CBL or CBL Mutants, ATP (Wild-Type 3.5 mM, CBL Mutants 7 mM) in 50 mM K^+HEPES Containing 16 mM $MgCl_2$ (pH 7.5, 25 °C)

CBL	$^{int}K_{eq}$	k_{obs} (s^{-1})	X-fold reduction in k_{obs}
wild-type	10	270 ± 10	
K492A	10	0.44 ± 0.04	600
R400A	10	1.7 ± 0.1	160
D385A	6	0.9 ± 0.1	300
T306A	6	61 ± 8	4
T307A	6	4.3 ± 0.3	60
T161A	10	0.070 ± 0.003	4000
H207A	7	3.0 ± 0.5	90
E410A	10	84 ± 0.04	3
R466A	10	210 ± 10	0
W440A	10	300 ± 40	0
F473A	10	400 ± 70	0

maximum accumulation of the [^{14}C]4-CB-AMP intermediate (calculated from the ratio of the [^{14}C]4-CB-AMP to the starting [^{14}C]4-CB). The two rate constants of particular interest are k_1 and k_2. The k_1 reflects the rate at which CBL(4-CB)(ATP) converts to CBL(4-CB-AMP)(PP_i). The k_2 reflects the rate at which the CBL(4-CB-AMP)(PP_i) complex releases PP_i and the CBL(4-CB-AMP) complex switches to conformation 2, binds CoA and then undergoes turnover to form the CBL(4-CB-CoA)(AMP) complex. The k_2 can be accurately defined only if the [^{14}C]4-CB-AMP intermediate accumulates during the single turnover reaction. This condition is met with the wild-type CBL catalyzed reaction, wherein the [^{14}C]4-CB-AMP accumulates to a level that corresponds to 70% of the starting [^{14}C]4-CB. The rate constants are well constrained at $k_1 = 300\ s^{-1}$ and $k_2 = 120\ s^{-1}$.

Third, the mutant CBL catalyzed single turnover reactions of [^{14}C]4-CB with ATP, and of [^{14}C]4-CB with ATP and CoA, were measured in order to evaluate the relative contributions of the targeted residues to partial reactions 1 and 2. The time courses for partial reaction 1 are shown in Figure SI2 (Supporting Information) and the k_{obs} and $^{int}K_{eq}$ values derived from these time courses are reported in Table 2. The time courses for the full reaction are shown in Figure 7C−G (for K492A CBL and W440A CBL for illustration of a time course dominated by a rate limiting first partial reaction and a time course dominated by a rate limiting second partial reaction, respectively) and in Figure SI3 (Supporting Information) (for R466A, E410A, F473A, R400A, D385A, T307A, H207A, and T161 CBL). The maximum level of [^{14}C]4-CB-AMP accumulation and the microscopic rate constants are reported in Table 3.

The suggested catalytic role of Lys492 is to bind the 4-CB carboxylate group. The K492A CBL mutant is severely impaired in catalysis of the first partial reaction. The [^{14}C]4-CB-AMP does not accumulate in the full reaction and therefore the rate constant for the second partial reaction cannot be defined by the computer based data simulations beyond: $k_2 > k_1$. The single turnover time course for the K492A CBL catalysis of the first partial reaction is shown in Figure 7C and the time course for the full reaction is shown in Figure 7D.

Thr307 forms a hydrogen bond with the 4-CB-AMP α-phosphate (Figure 6B), an interaction that is shown by the transient kinetic data to be more important to the first partial reaction (100-fold reduction in k_1) than to the second (~10-fold reduction in k_2) (Table 3). Like Thr307, Thr161 is observed to form a hydrogen bond to the 4-CB-AMP α-phosphate in the CBL(4-CB-AMP) structure (Figure 6B), yet whereas the T307A CBL mutant experiences a 60-fold reduction in the k_{obs} of the first partial reaction, the T161A mutant experiences a 4000-fold reduction in k_{obs} (Table 2). The difference in Thr307 and Thr161 contribution is consistent with an additional role played by the Thr161 (suggested by the position of the Thr161 counterpart in the structure of the human medium chain acyl-CoA synthetase(MgATP) complex) which is to bind the ATP γ-phosphate in the CBL(ATP)(4-CB) complex. The [^{14}C]4-CB-AMP does not accumulate during the single turnover of ATP, 4-CB and CoA and thus the rate constant for the second partial reaction cannot be defined by the computer based data simulations beyond: $k_2 > k_1$.

Asp385 and Arg400 each form a hydrogen bond with the AMP 2′-hydroxyl group in the CBL(4-CB-AMP) and CBL(4-CP-CoA)(AMP) structures (Figure 6B,C). These interactions may be required for both partial reactions. Indeed, both reactions are impaired in D385A CBL, however k_1 is reduced (400-fold) to greater extent than is k_2 (~20-fold). The k_1 is reduced 300-fold in the R400A mutant and the k_2 is reduced 100-fold. The 10-fold greater reduction observed in the R400A CBL k_2 vs the D385A CBL k_2 is consistent with the additional role that the Arg400 side chain assumes in catalysis which is stabilization of conformation 2 via ion pair formation with linker residue Asp402 (see Figure 6E).

The near equal reduction in k_1 (100-fold) and k_2 (150-fold) observed for H207A CBL is consistent with the suggested roles of the His207 side chain in binding the 4-CB carboxylate in the first partial reaction and stabilization of conformation 2 in the second partial reaction.

Residues thought to function only in the second partial reaction are W440, F473 and Glu410. In conformation 1 W440 and F473 are located on the solvated surface of the C-terminal domain whereas in conformation 2 these residues form the hydrophobic binding site for the CoA adenine ring (see green colored "stick" residues in Figure 2). In conformation 1, the Glu410 side chain is solvated, and in conformation 2 it enters the active site and forms a hydrogen bond with the His207 side chain, thereby stabilizing conformation 2 and thereby facilitating CoA binding (see Figure 6D). Consistent with the proposed roles of these three residues is the observation that Ala substitution has little or no impact on k_1 but reduces k_2 by 100 to 800-fold (Table 3).

The CBL Catalytic Mechanism. The CBL catalyzed formation of 4-CB-CoA is partitioned into two partial reactions (Figure 1), the first of which activates the 4-CB carboxylate group for the acyl transfer to CoA that takes place in the second partial reaction. The biochemical method of carboxylate group activation is nucleotidylation (or phosphorylation), a process in which a negatively charged carboxylate group undergoes nucleophilic attack at the phosphorus atom of a negatively charged phosphoryl group. The enzyme that catalyzes this type of reaction must employ electropositive groups to orient the carboxylate and phosphoryl groups for in-line attack, and to shield their point

Table 3: Microscopic Rate Constants Defined in Scheme 1 and Derived from Single Turnover Time Course Data (Shown in Figure SI2 of Supporting Information) for the Reaction of 8.3 μM [^{14}C]4-Chlorobenzoate with 29 μM Wild-Type CBL or CBL Mutant (Except T161A CBL which was 8.8 μM), ATP (Wild Type 3.5 mM, CBL Mutants 7 mM), CoA (1 mM Except for the R400A CBL Reaction it was 15 mM), and 16 mM $MgCl_2$ in 50 mM K^+HEPES (pH 7.5, 25 °C)[a]

	% EI	k_1 (s^{-1})	k_{-1} (s^{-1})	k_2 (s^{-1})	k_{-2} (s^{-1})	X-fold Step 1	X-fold Step 2
wild-type CBAL	70	300	0.01	120	0.1		
K492A[b]	0	0.24	0.41	*2*	*0.02*	1000	not defined
R400A	30	0.98	0.35	1.34	0.04	300	100
D385A	10	0.68	2.6	5.1	0.1	400	~20
T307A	10	3.0	5.0	12.0	0.1	100	~10
T161A[b]	0	0.05	0.1	*10*	*0.01*	6000	not defined
H207A	50	3.88	1.2	0.82	0.001	100	150
E410A	90	140	20	0.15	0.001	2	800
R466A	50	250	55	30	0.45	0	4
W440A	100	390	40	0.7	0.02	0	200
F473A	90	280	30	0.55	0.04	0	200

[a] The decrease in the microscopic rate constant that governs the conversion of CBL(4-CB)(ATP) to CBL(4-CB-AMP) in the mutant is reported in the X-fold Step 1 column, whereas the decrease in the microscopic rate constant that governs the conversion of CBL(4-CB-AMP)(CoA) to CBL(4-CB-CoA)(AMP) in the mutant is reported in the X-fold Step 2 column. [b] The rate constants for the second reaction cannot be accurately constrained by time course simulation because the CBL(4-CB-AMP)(PP_i) "EI" does not accumulate owing to the dramatic reduction in k_1.

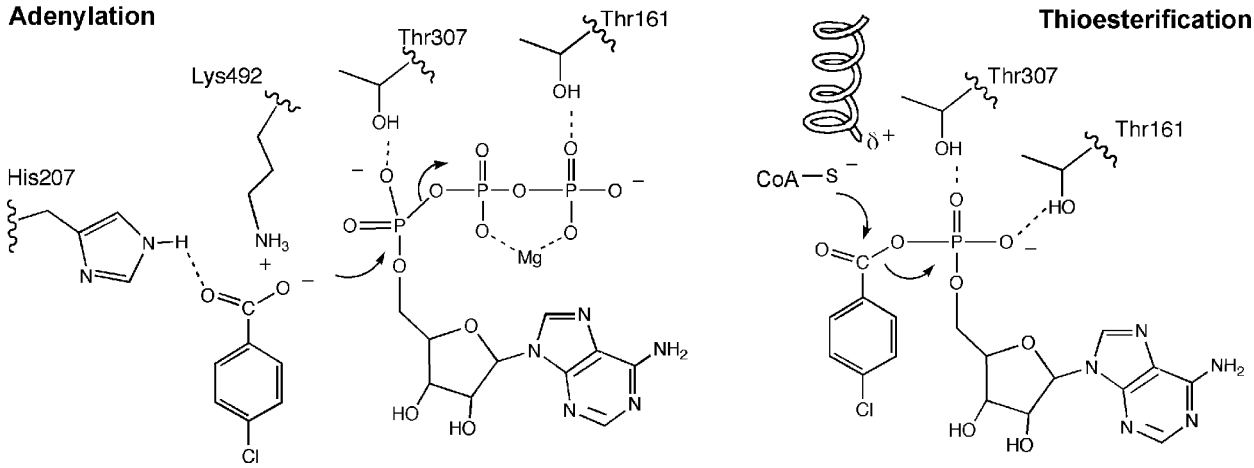

FIGURE 8: A depiction of the key catalytic residues and the role that they play in the adenylation step and/or the thioesterification step.

charges which, upon close encounter, would otherwise lead to unfavorable charge−charge interaction. The structural data reported in the accompanying paper (*17*) together with the CBL mutant kinetic data reported in this paper suggest that the catalytic residues which function in these two roles are Lys492 of the C-terminal domain, and His207 and Thr307 of the N-terminal domain (see Figure 8).

The leaving group of the nucleophilic substitution reaction is PP_i. The energy of this leaving group is reflected by the pK_a of the ionization of monoprotonated PP_i to the tetra-anion, which is 9.3. The departure of PP_i could be facilitated by acid catalysis. The Mg^{2+} cofactor (which is seen in the structure of the human medium chain acyl-CoA synthetase to form γ,β-bidentate complex with ATP, positioning the PP_i unit for in-line displacement) may function in this role in CBL catalysis. Such a role has strong precedent in adenylate cyclase, DNA polymerase and RNA polymerases (*33*–*35*). The P-loop is presumed to assist in orienting the PP_i unit for displacement.

The second partial reaction involves nucleophilic attack of the CoA thiol at the 4-CB-AMP carbonyl group with displacement of AMP. The structural and mutagenesis data suggest that the AMP unit is activated for displacement via the hydrogen bonds formed between the phosphoryl group oxygen atoms and the hydroxyl groups of Thr307 and Thr161. It is striking that the CBL structures offer no hint as to the identity of specific residues that could serve to activate the 4-CB-AMP carbonyl carbon and the CoA thiol during the nucleophilic substitution step. On the other hand, the electropositive N-terminus of the α-helix (Val208-Ala220) that is directed at the reaction center may reduce the pK_a of the CoA thiol (from 8.5) so that the thiolate anion is present under cellular conditions. In addition, the low energy of the AMP leaving group might facilitate concerted acyl transfer (*36*) thereby avoiding the formation of a tetrahedral oxyanion intermediate. The N-terminus of the α-helix (Val208-Ala220) may offer sufficient electrostatic interaction with the C═O to offset any partial charge build-up in the transition state.

The CBL catalytic mechanism is simplified through the use of several active site residues in more than a single function. Lys492 functions to activate the 4-CB carboxylate group for reaction with ATP while at the same time stabilizing CBL in conformation 1 as needed for catalysis of the first partial reaction. His207, on the other hand, functions in both partial reactions (first by activating 4-CB carboxylate group for reaction with ATP and second, by stabilizing the conformation that allows CoA to react with 4-CB-AMP) by switching between two positions in concert with the domain alternation (Figure 6D). Finally, Thr161 may interact with the departing PP_i in the first partial reaction and with phosphoryl group of the 4-CB-AMP in the second

partial reaction. This switch in position is possible owing to the location of the Thr161 on the mobile P-loop.

Domain Alternation and Residue Multitasking: A Common Strategy Among Members of the Acyl-adenylate Forming Superfamily? CBL is the first member of the acyl-adenylate forming superfamily to be observed via X-ray crystallographic analysis in the two domain-domain orientations (viz. conformer 1 and 2; Figure 2) that support catalysis of the two partial reactions which culminate in the conversion of a carboxylate metabolite to a thioester at the expense of ATP. The ping-pong kinetic mechanism observed for CBL can be understood within the structural changes that accompany the switch between conformers as required for catalysis of both partial reactions. The ping-pong kinetic mechanism has been reported for other family members and this suggests that they too employ domain alternation to catalyze the conversion of their carboxylate substrate to a thioester. Might they, like CBL, also use active site residues in more than one function? It is noteworthy that even though the acetyl-CoA synthetases utilize a Trp residue in place of the CBL His207 (as needed to help orient the acetate by filling the space of an otherwise too large pocket) the Trp residue switches its position as the acetyl-CoA synthetase switches from conformation 1 observed in the X-ray structure of the yeast acetyl-CoA synthetase (*12*) to conformation 2 observed in the X-ray structure of the bacterial acetyl-CoA synthetase (*4*).

The acyl-adenylate forming superfamily is an especially successful superfamily as evidenced by the large number of its members, and by the adaptation of the catalytic scaffold execute numerous, diverse biochemical functions. We believe that this success can be attributed to the efficiency in the utilization of the N-terminal domain to provide the binding sites for the three substrates and the C-terminal domain to provide the residues that serve to desolvate the respective catalytic sites, and to bind the two pairs of reactants. As we have observed with CBL, certain residues on the N-terminal domain and on the C-terminal domain are recruited to perform specialized functions in the catalysis of both partial reactions. This, and the timed alternation of the surfaces of the C-terminal domain to modify a single catalytic pocket for the two sequential half-reactions, suggests the honing of the collaboration between paired domain surfaces in catalysis. The picture of CBL catalysis that we have presented in this paper is no doubt only a "scratch on the surface" of an intricate web of interactions between residues that orchestrate the timing of domain-domain interface switches to keep in step with the rate of the respective chemical reactions. Future work will focus on the CBL domain-domain linker as it may play a pivotal role in domain alternation.

ACKNOWLEDGMENT

The authors wish to thank Al Mildvan for helpful discussion regarding the metal activation of enzymes catalyzing displacement of PP_i from ATP.

SUPPORTING INFORMATION AVAILABLE

Table listing k_{cat} and K_m values measured for wild-type and mutant CBL, and figures which depict double reciprocal plots kinetic data gathered for CBL dead-end and product inhibitors, time courses for a single turnover reactions of 4-chlorobenzoate and ATP catalyzed by mutant CBLs, and time courses for single turnover reactions of 4-chlorobenzoate, CoA and ATP catalyzed by mutant CBLs. This material is available free of charge via the Internet at http://pubs.acs.org.

REFERENCES

1. Babbitt, P. C., Kenyon, G. L., Martin, B. M., Charest, H., Slyvestre, M., Scholten, J. D., Chang, K. H., Liang, P. H., and Dunaway-Mariano, D. (1992) Ancestry of the 4-chlorobenzoate dehalogenase: analysis of amino acid sequence identities among families of acyl: adenyl ligases, enoyl-CoA hydratases/isomerases, and acyl-CoA thioesterases. *Biochemistry 31*, 5594–5604.
2. Scholten, J. D., Chang, K. H., Babbitt, P. C., Charest, H., Sylvestre, M., and Dunaway-Mariano, D. (1991) Novel enzymic hydrolytic dehalogenation of a chlorinated aromatic. *Science 253*, 182–185.
3. Turgay, K., Krause, M., and Marahiel, M. A. (1992) Four homologous domains in the primary structure of GrsB are related to domains in a superfamily of adenylate-forming enzymes. *Mol. Microbiol. 6*, 2743–2744.
4. Gulick, A. M., Starai, V. J., Horswill, A. R., Homick, K. M., and Escalante-Semerena, J. C. (2003) The 1.75 Å crystal structure of acetyl-CoA synthetase bound to adenosine-5′-propylphosphate and coenzyme A. *Biochemistry 42*, 2866–2873.
5. Reger, A. S., Carney, J. M., and Gulick, A. M. (2007) Biochemical and crystallographic analysis of substrate binding and conformational changes in acetyl-CoA synthetase. *Biochemistry 46*, 6536–6546.
6. Gulick, A. M., Lu, X., and Dunaway-Mariano, D. (2004) Crystal structure of 4-chlorobenzoate:CoA ligase/synthetase in the unliganded and aryl substrate-bound states. *Biochemistry 43*, 8670–8690.
7. Conti, E., Franks, N. P., and Brick, P. (1996) Crystal structure of firefly luciferase throws light on a superfamily of adenylate-forming enzymes. *Structure 4*, 287–298.
8. Conti, E., Stachelhaus, T., Marahiel, M. A., and Brick, P. (1997) Structural basis for the activation of phenylalanine in the nonribosomal biosynthesis of gramicidin S. *EMBO J. 16*, 4174–4183.
9. Wu, R., Reger, A. S., Cao, J., Gulick, A. M., and Dunaway-Mariano, D. (2007) Rational redesign of the 4-chlorobenzoate binding site of 4-chlorobenzoate: coenzyme a ligase for expanded substrate range. *Biochemistry 46*, 14487–14499.
10. Bains, J., and Boulanger, M. J. (2007) Biochemical and structural characterization of the paralogous benzoate CoA ligases from *Burkholderia xenovorans* LB400: defining the entry point into the novel benzoate oxidation (box) pathway. *J. Mol. Biol. 373*, 965–977.
11. Hisanaga, Y., Ago, H., Nakagawa, N., Hamada, K., Ida, K., Yamamoto, M., Hori, T., Arii, Y., Sugahara, M., Kuramitsu, S., Yokoyama, S., and Miyano, M. (2004) Structural basis of the substrate-specific two-step catalysis of long chain fatty acyl-CoA synthetase dimer. *J. Biol. Chem. 279*, 31717–31726.
12. Jogl, G., and Tong, L. (2004) Crystal structure of yeast acetyl-coenzyme A synthetase in complex with AMP. *Biochemistry 43*, 1425–1431.
13. May, J. J., Kessler, N., Marahiel, M. A., and Stubbs, M. T. (2002) Crystal structure of DhbE, an archetype for aryl acid activating domains of modular nonribosomal peptide synthetases. *Proc. Natl. Acad. Sci. U. S. A. 99*, 12120–12125.
14. Nakatsu, T., Ichiyama, S., Hiratake, J., Saldanha, A., Kobashi, N., Sakata, K., and Kato, H. (2006) Structural basis for the spectral difference in luciferase bioluminescence. *Nature 440*, 372–376.
15. Bandarian, V., Pattridge, K. A., Lennon, B. W., Huddler, D. P., Matthews, R. G., and Ludwig, M. L. (2002) Domain alternation switches B(12)-dependent methionine synthase to the activation conformation. *Nat. Struct. Biol. 9*, 53–56.
16. Chang, K. H., and Dunaway-Mariano, D. (1996) Determination of the chemical pathway for 4-chlorobenzoate:coenzyme A ligase catalysis. *Biochemistry 35*, 13478–13484.
17. Reger, A. S., Wu, R., Dunaway-Mariano, D., and Gulick, A. M. Structural Characterization of a 140° domain movement in the two-step reaction catalyzed by 4-chlorobenzoate:CoA ligase*Biochemistry 47*, 8016–8025.
18. Wu, R. Domain movement and substrate recognition in 4-chlorobenzoate: coenzyme A ligase from Alcaligenes sp strain AL3007. Ph.D. Thesis, University of New Mexico, pp 36–38.

19. Bradford, M. M. (1976) A rapid and sensitive method for the quantitation of microgram quantities of protein utilizing the principle of protein-dye binding. *Anal. Biochem. 72*, 248–254.
20. Chang, K. H., Xiang, H., and Dunaway-Mariano, D. (1997) Acyl-adenylate motif of the acyl-adenylate/thioester-forming enzyme superfamily: a site-directed mutagenesis study with the Pseudomonas sp. strain CBS3 4-chlorobenzoate:coenzyme A ligase. *Biochemistry 36*, 15650–15659.
21. Barshop, B. A., Wrenn, R. F., and Frieden, C. (1983) Analysis of numerical methods for computer simulation of kinetic processes: development of KINSIM−a flexible, portable system. *Anal. Biochem. 130*, 134–145.
22. Horswill, A. R., and Escalante-Semerena, J. C. (2002) Characterization of the propionyl-CoA synthetase (PrpE) enzyme of *Salmonella enterica*: residue Lys592 is required for propionyl-AMP synthesis. *Biochemistry 41*, 2379–2387.
23. Martínez-Blanco, H., Reglero, A., Rodriguez-Aparicio, L. B., and Luengo, J. M. (1990) Purification and biochemical characterization of phenylacetyl-CoA ligase from Pseudomonas putida. A specific enzyme for the catabolism of phenylacetic acid. *J. Biol. Chem. 265*, 7084–7090.
24. Kwon, O., Bhattacharyya, D. K., and Meganathan, R. (1996) Menaquinone (vitamin K2) biosynthesis: overexpression, purification, and properties of O-succinylbenzoyl-coenzyme A synthetase from *Escherichia coli*. *J. Bacteriol. 178*, 6778–6781.
25. An, J. H., Lee, G. Y., Jung, J. W., Lee, W., and Kim, Y. S. (1999) Identification of residues essential for a two-step reaction by malonyl-CoA synthetase from *Rhizobium trifolii*. *Biochem. J. 344*, 159–166.
26. Bar-Tana, J., and Rose, G. (1968) Studies on medium-chain fatty acyl-coenzyme a synthetase. Enzyme fraction I: mechanism of reaction and allosteric properties. *Biochem. J. 109*, 275–282.
27. Berg, P. (1956) Acyl adenylates: an enzymatic mechanism of acetate activation. *J. Biol. Chem. 222*, 991–1013.
28. Branchini, B. R., Murtiashaw, M. H., Magyar, R. A., and Anderson, S. M. (2000) The role of lysine 529, a conserved residue of the acyl-adenylate-forming enzyme superfamily, in firefly luciferase. *Biochemistry 39*, 5433–5440.
29. Hamoen, L. W., Eshuis, H., Jongbloed, J., Venema, G., and van Sinderen, D. A. (1995) A small gene, designated comS, located within the coding region of the fourth amino acid-activation domain of srfA, is required for competence development in *Bacillus subtilis*. *Mol. Microbiol. 15*, 55–63.
30. Branchini, B. R., Magyar, R. A., Murtiashaw, M. H., Anderson, S. M., Helgerson, L. C., and Zimmer, M. (1999) Site-directed mutagenesis of firefly luciferase active site amino acids: a proposed model for bioluminescence color. *Biochemistry 38*, 13223–13230.
31. Zhuang, Z., Song, F., Zhang, W., Taylor, K., Archambault, A., Dunaway-Mariano, D., Dong, J., and Carey, P. R. (2002) Kinetic, Raman, NMR, and site-directed mutagenesis studies of the *Pseudomonas* Sp. strain CBS3 4-hydroxybenzoyl-CoA thioesterase active site. *Biochemistry 41*, 11152–11160.
32. Luo, L., Taylor, K. L., Xiang, H., Wei, Y., Zhang, W., and Dunaway-Mariano, D. (2001) Role of active site binding interactions in 4-chlorobenzoyl-coenzyme A dehalogenase catalysis. *Biochemistry 40*, 15684–15692.
33. Brautigan, C. A., and Steitz, T. A. (1998) Structural and functional insights provided by crystal structures of DNA polymerases and their substrate complexes. *Curr. Opin. Struct. Biol. 8*, 54–63.
34. Doublie, S., and Ellenberger, T. (1998) The mechanism of action of T7 DNA polymerase. *Curr. Opin. Struct. Biol. 8*, 704–712.
35. Tesmer, J. J., Sunahara, R. K., Johnson, R. A., Gosselin, G., Gilman, A. G., and Sprang, S. R. (1999) Two-metal-ion catalysis in adenylyl cyclase. *Science 285*, 756–760.
36. Hess, R. A., Hengge, A. C., and Cleland, W. W. (1998) Isotope effects on enzyme catalyzed acyl transfer from *p*-nitrophenylacetate: concerted mechanisms and increased hyperconjugation in the transition state. *J. Am. Chem. Soc. 120*, 2703–2709.

BI800698M